Supporting Information

Defect Compensation and Intervalence Charge Transfer State-Based Pr^{3+}-Doped Niobate Antithermal Quenching Phosphors

Chunwei Yang,[a] Yanmei Xin,[a] Jianxia Liu,[a] Yuefeng Zhao,[a] Ruizhuo Ouyang[a] and Ning Guo[*a]

[a] Department of Chemistry, University of Shanghai for Science and Technology, Shanghai 200093, P. R. China.

*Corresponding author: E-mail: guoning@usst.edu.cn

1.Experimental Section

1.1. Materials and Synthesis.

A series of $Sr_{2-x}Ca_xNb_2O_7$:Pr^{3+}(0.5%) (x = 0, 0.5, 1.0, 1.5, 2.0) phosphors were prepared using a high-temperature solid-state method. All samples were prepared with $SrCO_3$ (99.9%), $CaCO_3$ (99.9%), Nb_2O_5 (99.9%), and P_6O_{11} (99.9%) as raw materials, accurately weighed according to the stoichiometric ratio, and 0.5% Li_2CO_3 (99.9%) was added as a co-solvent. During the preparation process, the mixture was thoroughly ground for 30 minutes in an agate mortar, then transferred to a covered crucible, and react in air at 900°C for 4 h, then grind for 30min, then transfer to air at 1400°C for 4 h. The final product was cooled to room temperature and ground again for 30 minutes for subsequent analysis.

1.2. Characterization Methods.

The samples were tested by X-ray diffraction (XRD), XRD Rietveld refinements, scanning electron microscopy (SEM), Raman spectra, UV-vis diffuse reflectance spectroscopy, X-ray Photoelectron Spectroscopy (XPS), thermoluminescence (TL) spectrum, photoluminescence excitation (PLE) spectra, photoluminescence (PL) spectra, and temperature-dependent spectra. The TL spectrum was measured by TOSL-3DS instrument, excited at 254 nm for 5 min, and then heated at 1 K/s. For detailed information and parameters of the other tests, please refer to our previous work.[1, 2]
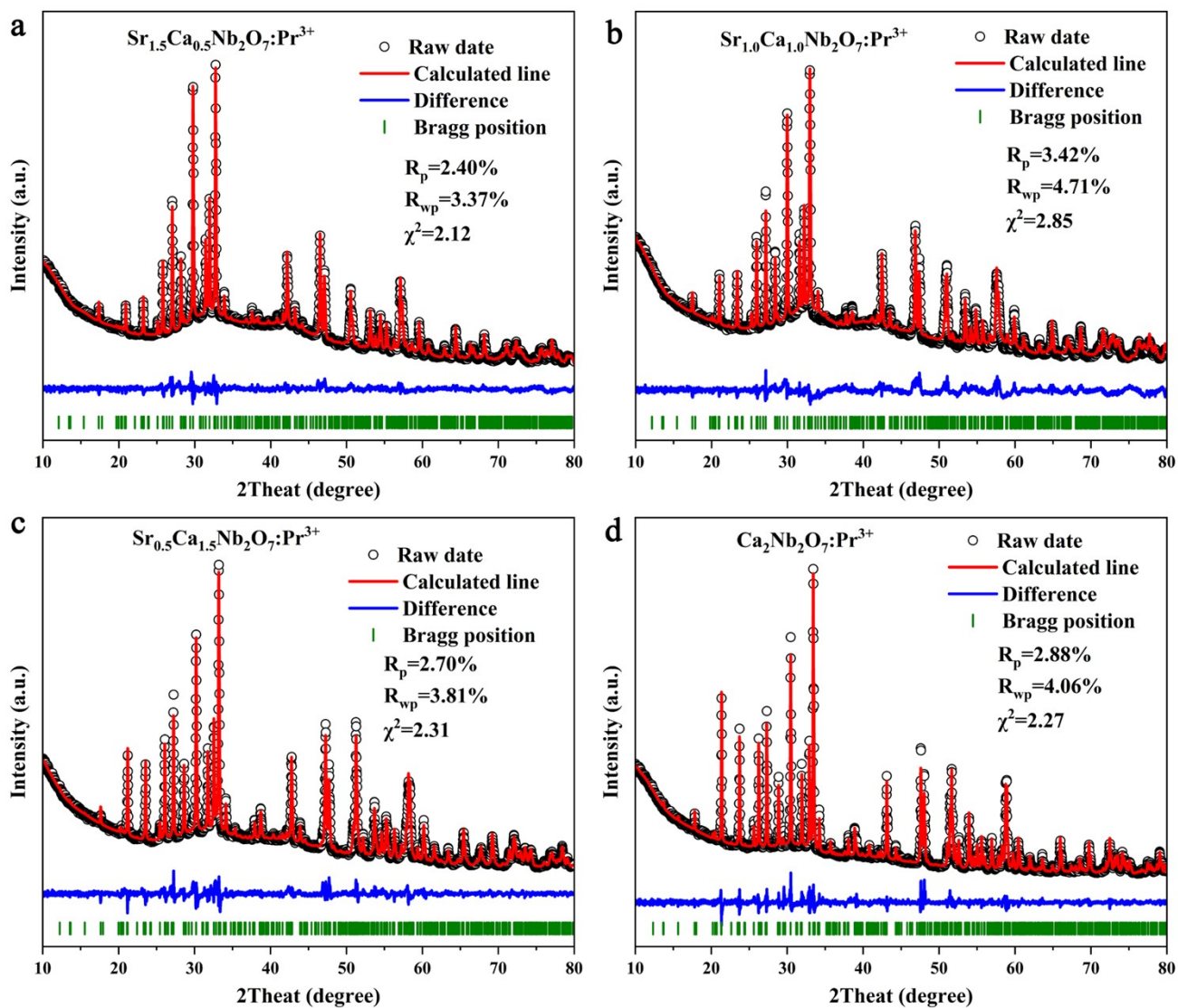
Figure S1

Figure S1. The Rietveld refinement plot of the X-ray diffraction pattern of $Sr_{2-x}Ca_xNb_2O_7:Pr^{3+}$ (x = 0.5, 1.0, 1.5, 2.0).
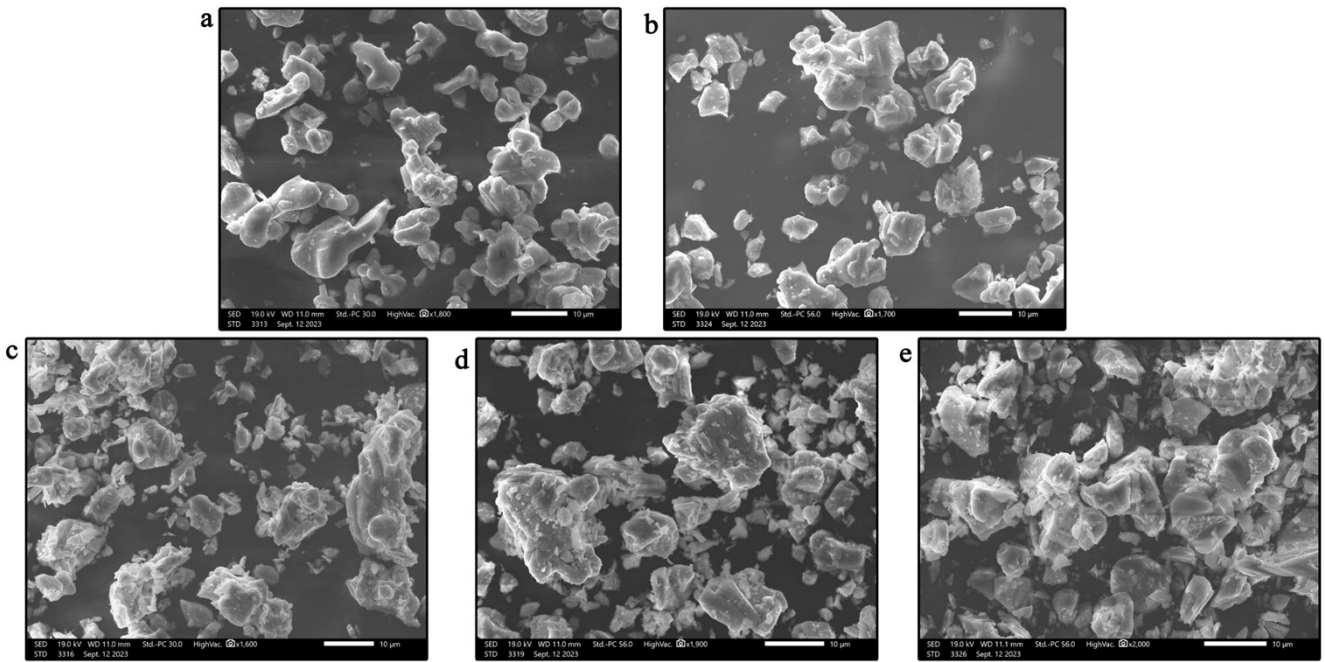
Figure S2

Figure S2. The SEM image of $Sr_{2-x}Ca_xNb_2O_7:Pr^{3+}$ (a) x = 0, (b) x= 2.0, (c) x=0.5, (d) x=1.0, (e) x=1.5.

Figure S3

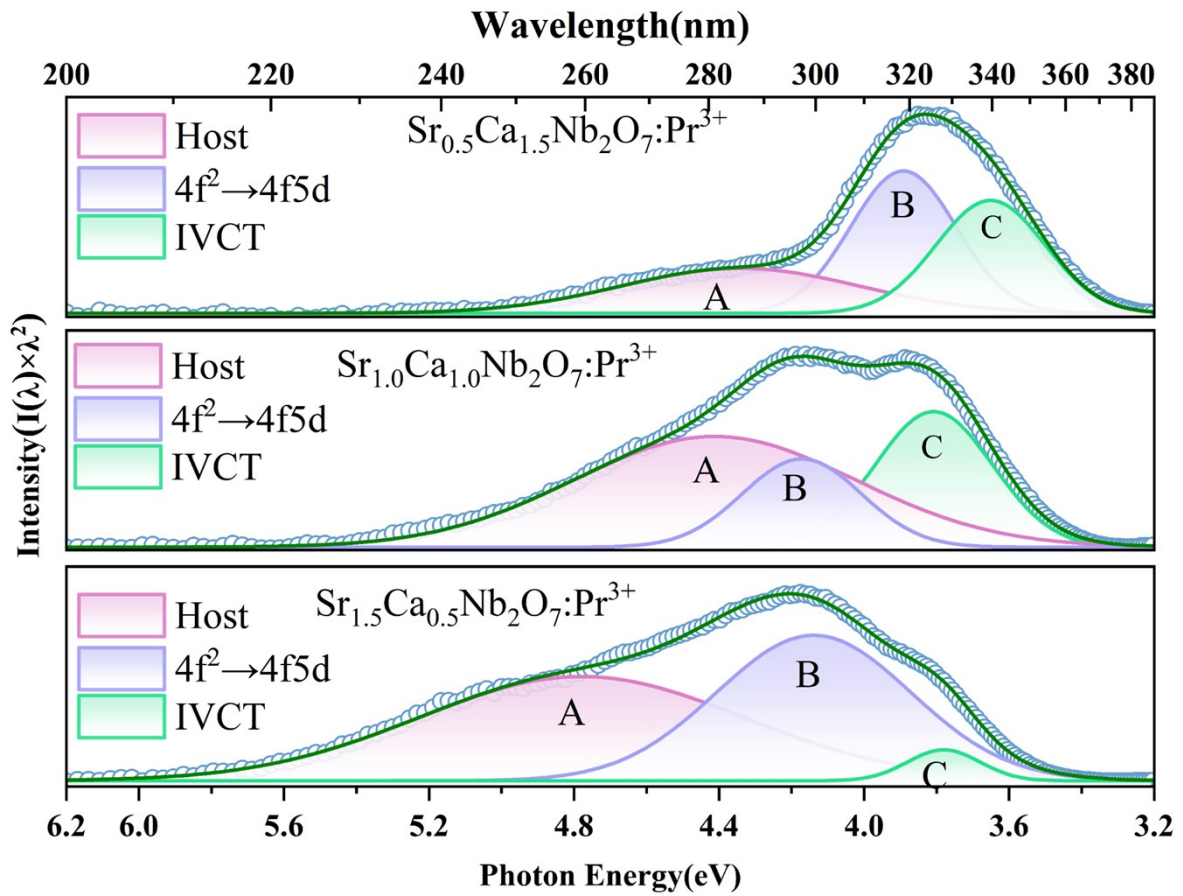

Figure S3. Gaussian fitting to the photoluminescence excitation spectrum of $Sr_{1.5}$, $Sr_{1.0}$, $Sr_{0.5}$.

Figure S4

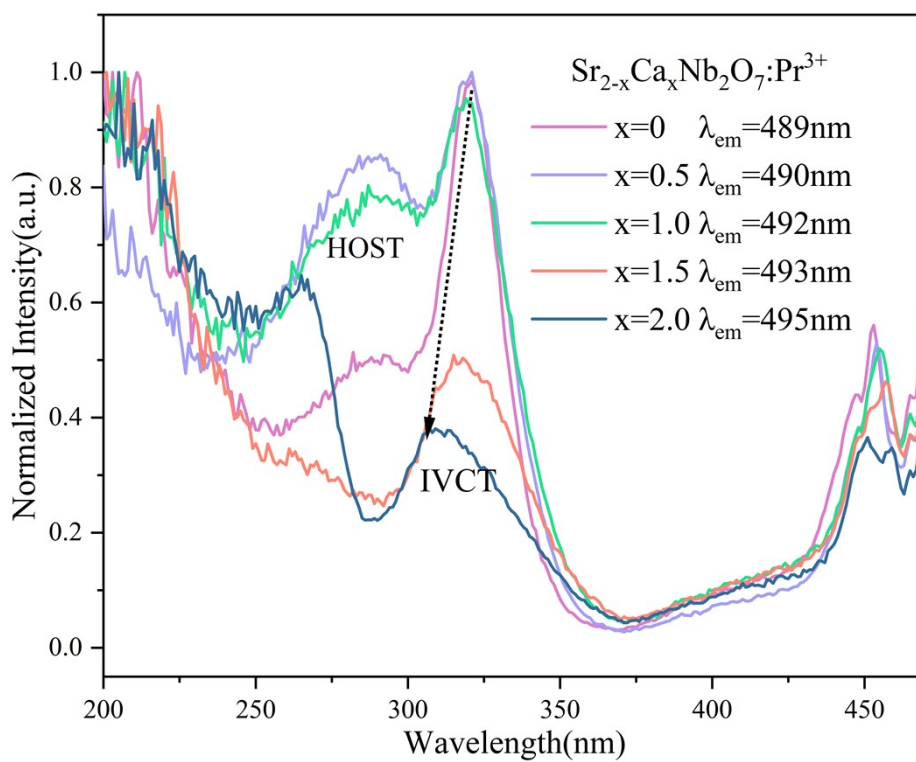Figure S4. Monitoring the normalized PLE spectra of $Sr_{2-x}Ca_xNb_2O_7$:Pr^{3+} (x = 0, 0.5, 1.0, 1.5, 2.0) for the $^3P_0 \rightarrow {}^3H_4$ emission.

Figure S5
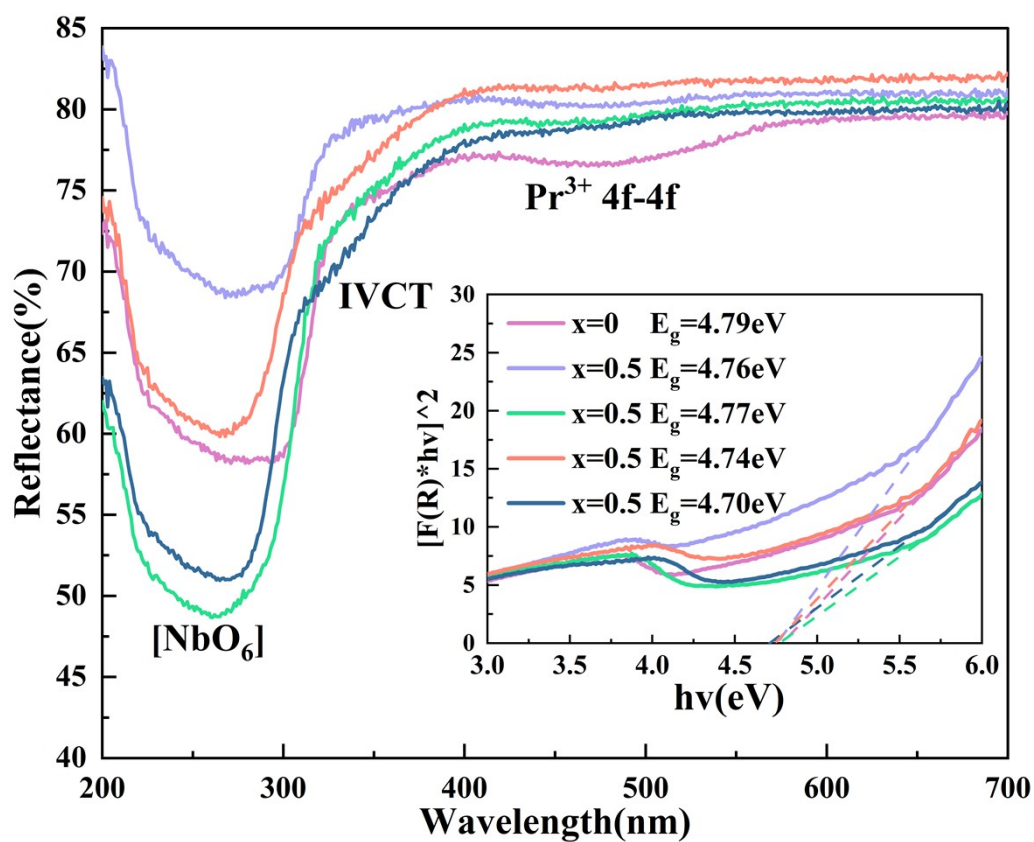

Figure S5. DR spectra of $Sr_{2-x}Ca_xNb_2O_7$:Pr^{3+} (x = 0, 0.5, 1.0, 1.5, 2.0). The illustration in the lower right corner is the energy-gap value of $Sr_{2-x}Ca_xNb_2O_7$:Pr^{3+} (x = 0, 0.5, 1.0, 1.5, 2.0) calculated according to the Kubelka−Munk absorption function.
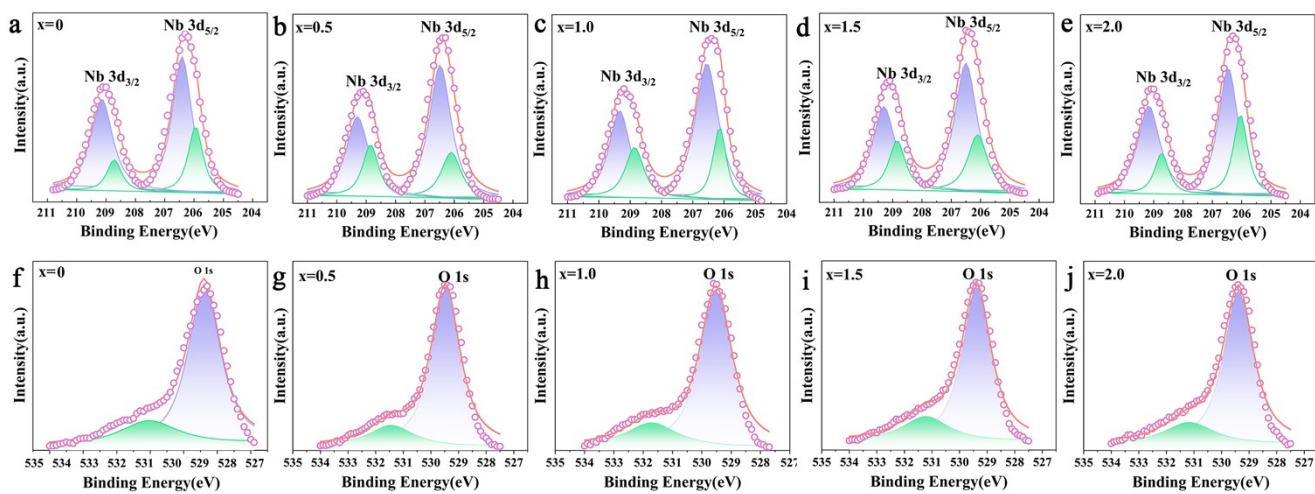
Figure S6

Figure S6. XPS spectra of Nb 3d (a-e) and O 1s (f-j) of $Sr_{2-x}Ca_xNb_2O_7:Pr^{3+}$ (x = 0, 0.5, 1.0, 1.5, 2.0).

Figure S7
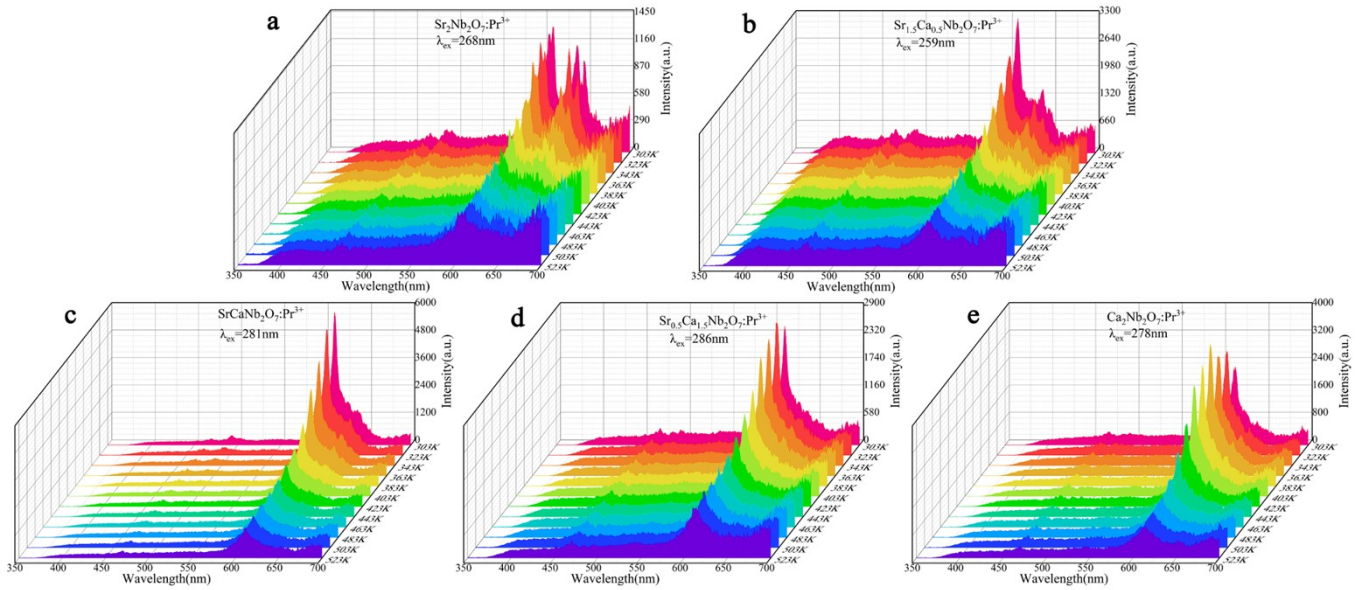

Figure S7. Temperature-dependent PL spectra of $Sr_{2-x}Ca_xNb_2O_7$:Pr^{3+} (x = 0, 0.5, 1.0, 1.5, 2.0) under excitation at CTB.

Figure S8
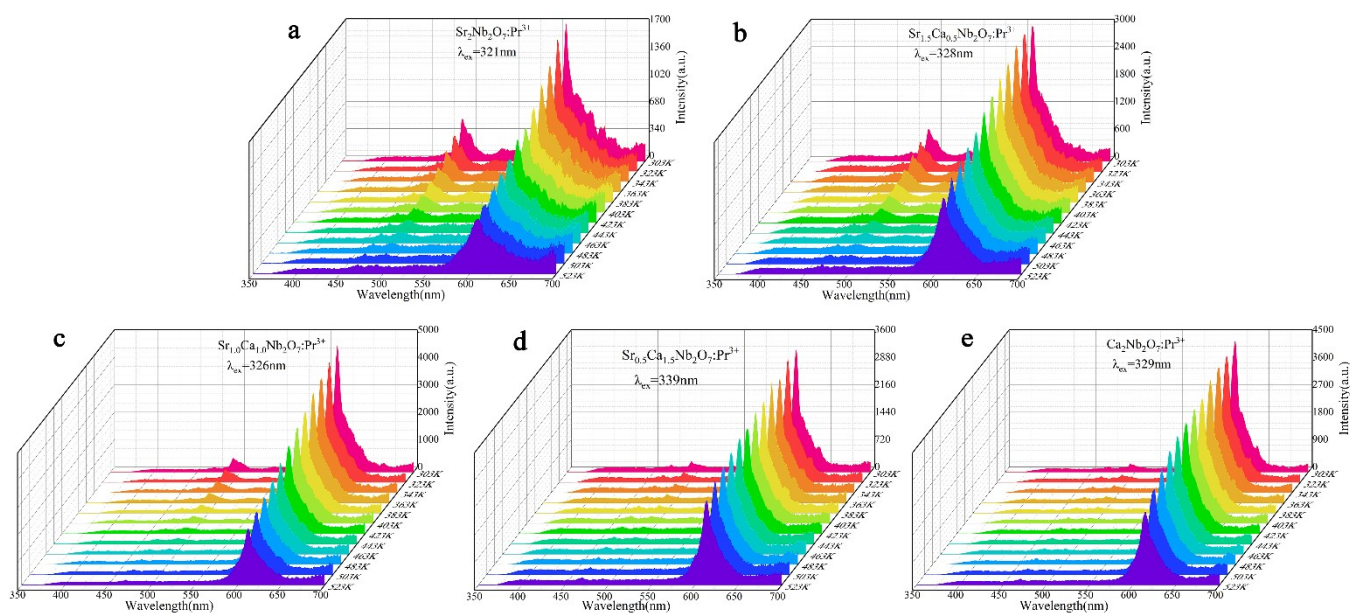

Figure S8. Temperature-dependent PL spectra of $Sr_{2-x}Ca_xNb_2O_7:Pr^{3+}$ (x = 0, 0.5, 1.0, 1.5, 2.0) under excitation at IVCT band.

Figure S9
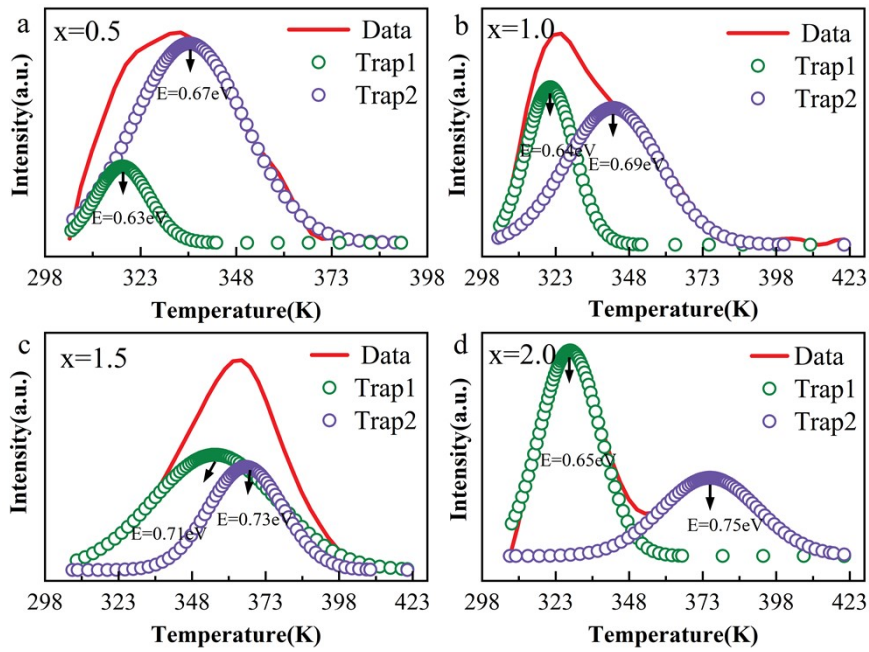
Figure S9. The Gaussian fit of TL curve of $Sr_{2-x}Ca_xNb_2O_7$:Pr^{3+} (x = 0.5, 1.0, 1.5, 2.0).

Figure S10
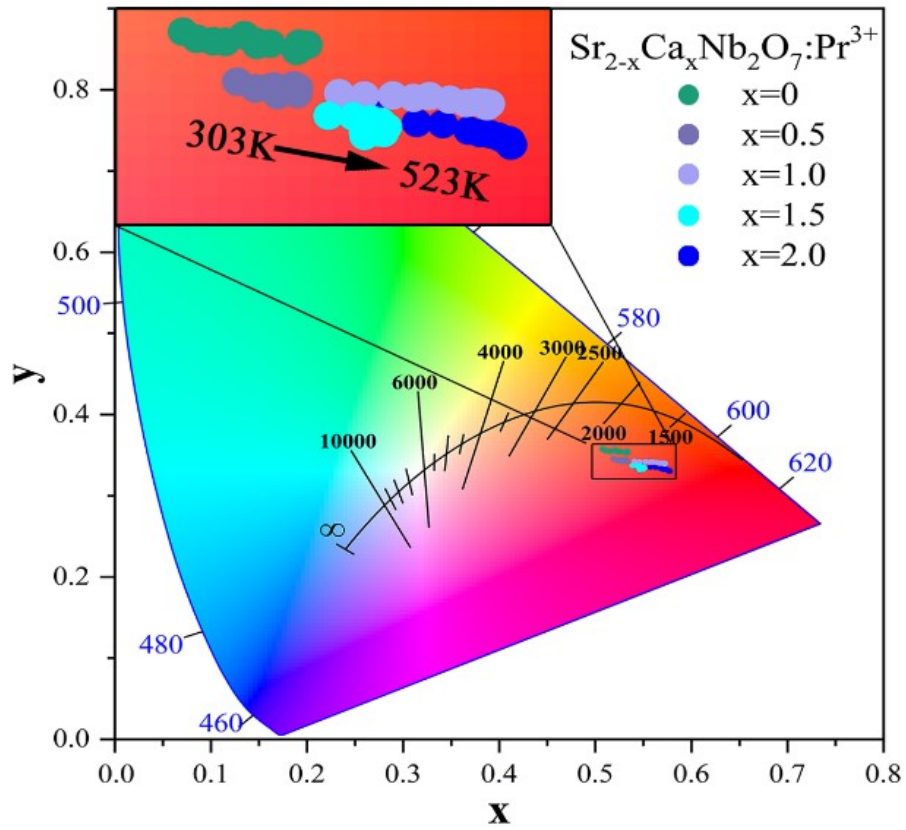

Figure S10. The CIE chromaticity diagram and CIE coordinate shift of $Sr_{2-x}Ca_xNb_2O_7:Pr^{3+}$ (x = 0, 0.5, 1.0, 1.5, 2.0) at different temperatures under IVCT band excitation.

Table S1

Table S1. Refinement results of the atomic coordinates of $Sr_{2-x}Ca_xNb_2O_7$:Pr^{3+} (x = 0, 0.5, 1.0, 1.5, 2.0).

parameter	space group	a(Å)	b(Å)	c(Å)	$\alpha = \beta = \gamma$(°)	V(Å^3)
$Sr_{2.0}$	Pna21	26.7768(3)	7.90949(8)	5.70105(7)	90	1207.428(17)
$Sr_{1.5}$	Pna21	26.7081(5)	7.85923(13)	5.66048(12)	90	1188.17(3)
$Sr_{1.0}$	Pna21	26.5977(8)	7.80319(19)	5.61555(17)	90	1165.49(4)
$Sr_{0.5}$	Pna21	26.5096(5)	7.74092(13)	5.55500(12)	90	1139.936(26)
Sr_0	Pna21	26.4426(4)	7.68791(9)	5.49584(8)	90	1117.242(18)

Table S2

Table S2. IVCT Energy Level Positions Calculated According to Theoretical Empirical Formulas.

Sample	$Sr_{2.0}$	$Sr_{1.5}$	$Sr_{1.0}$	$Sr_{0.5}$	Sr_0
$d_{min}(Pr^{3+}-Nb^{5+})$ (Å)	3.4107	3.2548	3.3797	3.2155	3.2922
Wavenumber (cm^{-1})	31788.27	30494.11	31540.10	30148.51	30815.33
Wavelength (nm)	315	328	317	332	325
Theoretical equation	$IVCT(cm^{-1}) = 58800 - 49800\left[\dfrac{\chi_{opt}(Nb^{5+})^*}{d_{min}(Pr^{3+}-Nb^{5+})}\right]$				

*χ_{opt} is the Nb^{5+}optical electronegativity (Nb^{5+} = 1.85).[3]

References

1.   C. Yang, et al., *Inorg. Chem. Front.*, 2023, **10**, 4808-4818.
2.   X. Lv, et al., *J. Lumin.*, 2023, **255**, 119609.
3.   P. Boutinaud, et al., *J. Phys.: Condens. Matter*, 2007, **19**, 386230.